RELATIONSHIPS OF AGONIST PROPERTIES TO THE SINGLE CHANNEL KINETICS OF NICOTINIC ACETYLCHOLINE RECEPTORS

ROGER L. PAPKE, GLENN MILLHAUSER, ZORBA LIEBERMAN, AND ROBERT E. OSWALD
Department of Pharmacology, College of Veterinary Medicine, Cornell University, Ithaca, New York 14853

ABSTRACT The effects of the systematic variations of the acetylcholine molecule on the microscopic kinetics of channel activation were studied using the patch clamp technique. The modifications consisted of adding either halogens or a methyl group to the acetyl carbon of acetylcholine, which results in a change in both the steric and ionic character of that portion of the molecule. The ionic character of the bond affected both the opening and closing rates of the channel. An increase in the ionicity decreased the opening rate and increased the closing rate of the channel, suggesting that the open state was destabilized. Increasing the size of the substituent decreased both the association and dissociation rates for agonist binding but had little effect on the equilibrium constant. This indicates that the energy barrier for binding and unbinding was increased without a major change in the energy of the bound and unbound states. These results suggest that it is possible to assign changes in the structural characteristics of the ligand to changes in individual steps in a reaction scheme, which can lead to specific predictions for the properties of related compunds.

INTRODUCTION

The nicotinic acetylcholine receptor (AChR)[1] from *Torpedo* electroplaque and skeletal muscle tissue is a multisubunit complex consisting of four different types of glycosylated subunits with protein molecular weights (Claudio et al., 1983; Devillers-Thiéry et al., 1983; Noda et al., 1983) of 50,116 (α), 53,681 (β), 56,279 (γ), and 57,565 (δ), existing in a monomer stoichiometry of $\alpha_2\beta\gamma\delta$ (Reynolds and Karlin, 1978; Lindstrom et al., 1979; Raftery et al., 1980). These components are necessary and sufficient for mediation of channel opening by the AChR as determined by injection of mRNA coding for each subunit into *Xenopus* oocytes (Mishina et al., 1985; Sakmann et al., 1985; White et al., 1985).

Structure–function relationships on the level of the receptor protein are being pursued with great success in a number of laboratories using either site-directed mutagenesis (Mishina et al., 1985) or affinity labeling followed by peptide isolation and gas phase sequencing (Kao et al., 1984; Giraudat et al., 1986; Hucho et al., 1986). These studies have identified specific amino acids that interact with acetylcholine (ACh) and noncompetitive blockers (Kao et al., 1984; Giraudat et al., 1986; Hucho et al., 1986) as well as specific amino acids that seem to be involved in determining the conductance of the ion channel (Imoto et al., 1986).

A complementary approach to understanding the chemical gating of an ion channel is to study the structure–function relationships of the agents that activate the channel. Model studies using relatively small synthetic "receptors" have shown clearly that complementarity between the size, shape, and functional groups of the binding site and the ligand are critical for molecular recognition (see review by Rebek, 1987). This suggests that much information can be obtained concerning the structure of the binding site and the relationship of the structure of the ligand to the activity of the protein by studying the effects of systematic structural modifications of the ligand on the activity of a receptor protein. Traditionally, quantitative structure–activity relationships have been generated using macroscopic kinetic parameters (review in Hansch, 1983). While such an approach has provided important information on the structural requirements of channel activation (e.g., Spivak et al., 1983, 1986), detailed studies of microscopic kinetics are required for understanding the structural basis of individual steps in a reaction scheme. The introduction of the single channel recording technique (Neher and Sakmann, 1976; Hamill et al., 1981) has made possible the measurement of the fluctuations of single protein molecules, which, in some cases, allows the direct determination of microscopic kinetic parameters. By treating the transitions between

Please address correspondence to Robert E. Oswald, Department of Pharmacology, College of Veterinary Medicine, Cornell University, Ithaca, New York 14853.

[1] *Abbreviations used in this paper:* ACh, acetylcholine; AChR, acetylcholine receptor; α-Bgt, α-bungarotoxin; BrACh, bromoacetylcholine; ClACh, chloroacetylcholine; FACh, fluoroacetylcholine; PrCh, propionylcholine.

individual receptor states as first order or pseudofirst order rate constants and assuming Markovian behavior, individual microscopic rate constants for ACh binding and channel activation can be assigned with a minimum of assumptions (Colquhoun and Hawkes, 1981, 1982, 1983; Sine and Steinbach, 1986, 1987).

We have prepared a series of ACh derivatives with systematic modifications of the acetyl moiety. In each case, the added substituent consists either of a halogen or methyl group. These modifications vary both the ionic character of the bond and the length of the bond (which is in turn related to steric factors). Using single channel recording of AChRs from a mouse clonal muscle-like cell line (BC_3H-1), we show that the energy barrier for binding of ACh derivatives is increased by increasing bond length of the substituent and that the open channel state is destabilized by increasing ionicity of the substituent bond.

MATERIALS AND METHODS

Maintenance of Cell Line

BC_3H-1 cells were grown and maintained in Dulbecco's modified Eagle's medium with 10% fetal calf serum (without antibiotics) at 37°C in 10% CO_2. For single channel recording experiments, cells were pelleted, resuspended in growth medium, and plated on 35-mm dishes. After 1 d, the cells were rinsed with a low serum medium (0.5% fetal calf serum) and then maintained in the same medium to induce differentiation (Olsen et al., 1983). Cells were used 10–18 d after the serum change with medium changes every 5 d.

Single Channel Recording

The cell-attached recording configuration described by Hamill et al. (1981) was used in all cases. A modified Ringer's solution (room temperature) consisting of 147 mM NaCl, 5.4 mM KCl, 1 mM $MgCl_2$, and 10 mM Hepes was used both in the bathing medium and inside the pipette. ACh or other agonists were added to the pipette solution at a concentration of 100 nM. Additionally, 4.0 μM tetrodotoxin (TTX) was included in the pipette. TTX increased both the stability of the recordings and the signal-to-noise ratio, possibly by decreasing the activity of a low conductance cationic channel (such as an embryonic Na^+ channel). Firepolished pipettes of 4–8 MΩ were constructed from borosilicate glass (TW150-4; W.P. Instruments, New Haven, CT) and were coated within 50 μm of the tip with Sylgard. Dagan patch clamp electronics (10 GΩ probe) were used. In most cases, recordings were made at 80 mV hyperpolarized relative to resting potential. Variations in the resting potentials were reflected in the differences in the current amplitude observed at a holding potential of 0 mV. The range for these currents was 0.5–1.75 pA, corresponding to a range in the resting potentials of ~30 mV (assuming a constant relationship between reversal potential and resting potential). This variability was the same for all of the agonists studied; and therefore, variations in resting potentials should be statistically averaged out and reflected in the error estimates. Drift in the resting potential over the course of a recording was not a problem since a recording was analyzed only if the current amplitude did not change (which would be consistent with the patch detaching or a resting potential shift).

The data were electronically filtered (Krohn-Hite Corp., Avon, MA) at 10 kHz and stored on FM tape (15 in./s). The tape was played back at a fourfold lower speed, and the data were digitized at an effective rate of 40 kHz using a PDP 11/24 computer (AR11 analog-to-digital converter). The data collection software, written in assembly language, was run under the RSX11M operating system (interrupts were disabled by setting the maximum priority and turning off the line clock). Channels were viewed on a monitor before inclusion in the analysis and were detected by a simple threshold crossing algorithm with hysteresis. That is, the algorithm for event detection required that the current amplitude cross a level that was a certain increment above the half maximum current level, in order for the channel to be considered open, and that the current amplitude cross a threshold the same increment below the half maximum current level for it to be considered closed. The increment (Hysteresis factor) was approximately equal to 1/2 the open channel noise (at 10 kHz) and provided symmetrical criteria for the detection of fast opening and closures. The t_{min} was empirically determined for the response of our recording and detection system using this algorithm. In some cases, the traces were also stored in digital format (44.1 kHz sampling rate) on a video cassette recorder using a pulse code modulator (PCM; Unitrade Inc., Philadelphia, PA). The data were then transferred directly to the PDP 11/24 using the parallel output on the PCM and a DRU11-cc DMA parallel input on the computer.

Data Analysis

The length of the open and closed events were analyzed on MicroVAX I and II computers (FORTRAN-77 programs developed in the laboratory) by fitting to one-, two-, three, and four-exponential models with a Simplex algorithm (Caceci and Cacheris, 1984) using the maximum likelihood criterion (Colquhoun and Sigworth, 1983) for convergence. The response of our recording and analysis system was tested empirically, and the minimum dwell time that could be accurately measured was 50 μs. The records were corrected for unresolvable events as described by Colquhoun and Sigworth (1983; see also Colquhoun and Sakmann, 1981). In the analysis of records, any dwell times <50 μs were discarded and the probability density functions fit only to those events >50 μs.

Pooling data obtained under identical conditions was necessary, however, the distributions obtained from different records were analyzed independently. The reported values of β and k_{-2} are the average of single records so that the errors reported reflect the variation in the parameters calculated for different patches. Only the calculation of k_+ required the value for AChR site density and hence incorporates a greater number of sources of error. Values reported represent the means ± SEM for the fits of 4–11 (usually 5–8) records obtained under the same experimental conditions. For purposes of display, burst and closed distributions were presented as histograms. In the case of closed time histograms, a logarithmic transform of time was used on the abscissa in order to represent all relevant portions of the distribution. As shown by Sigworth and Sine (1987), the time constants for each exponential are represented by peaks in the distribution.

Calculation of Burst Durations

In general, channel openings occurred in groups of one or more which have been referred to as "bursts" (Sakmann et al., 1980). Burst durations were determined by choosing a time interval below which all closing intervals would be considered closures within a burst. The burst duration was then defined as the time between the opening of the first channel within the burst and the closure of the last channel within the burst. The time interval for defining a closure within a burst was determined by systematically testing 50 intervals between 0 and 20 ms and calculating the mean "burst duration" for one- and two-exponential models for each interval. The time constants for the burst duration distributions were then plotted as a function of the time interval. In all cases, the closures within a burst were much shorter than closures between burst, so that the calculated time constants reached a plateau. The time interval determining a closure within a burst was then defined as the first point after which the plateau occurred (typically 1 ms).

Correction for Missed Events

Assuming all single events could be resolved, the reciprocal of the mean channel lifetime should equal the closing rate of the channel (α). In

practice, rapid, unresolved closures bias the measurement of the mean channel lifetime so as to produce artifactually long open times. A correction for these missed unresolved closures was obtained by using the number of short closures (τ_{cl}; see Results), corrected for missed short closures. Our correction for the number of missed events was based on the extrapolation of the closed time distributions between t_{min} and zero. To obtain an estimate of α and the number of fast closures per burst, we estimated the true mean channel lifetime as described below (excluding any class of closures faster than our observed τ_{cl}).

As described in the Results, the burst duration histogram was, in all cases, a double exponential distribution, which complicated somewhat the correction for missed short closures. The majority of short closures occurred within long bursts, but some were also associated with short bursts. To estimate the short closures within long bursts, it was necessary to correct for the short closures that occurred between short openings. This correction was made based on the relative effect of burst analysis on the two types of bursts. If burst analysis produced a distribution in which the duration of short bursts was the same as that of short openings (as was the case with fluoroacetylcholine [FACh]), then no short closures were assumed to be associated with short openings. If, on the other hand, the short component of the burst distribution was longer than the short open time, then a percentage of short closures was assumed to be associated with the short bursts. The relative number of such short closures associated with the two types of bursts was estimated as the ratio of the relative increases in burst durations-to-open times for the two classes of events (long and short bursts). For example, if the short bursts were only 10% longer than short openings and long bursts were 50% longer than long openings, long bursts (relative to short bursts) were assumed to have five times more short closures. This ratio was then used to calculate the total number of short closures in short bursts. In the example above, if half of all bursts were short and (relative to long bursts) had one-fifth as many short closures, then one-sixth of all short closures were associated with short bursts. The total number of short closures, from the fit of the closed time distribution, could then be corrected to subtract those that occurred within short bursts to give the number of short closures within long bursts. This value was then divided by the number of long bursts to give the number of short closures per long burst. The open time was determined by dividing the mean burst duration by the number of openings per burst (one plus the number of short closures per burst). This resulted in faster closing rates (α) than those calculated from apparent open times (17% greater for propionylcholine [PrCH], 21% greater for FACh, 36% greater for ACh, 70% greater for bromoacetylcholine [BrACh], and 73% greater for chloroacetylcholine [ClACh]).

Preparation of Halogenated Derivatives of ACh

BrACh was prepared as described by Damle et al. (1978). The syntheses of FACh and ClACh are given below.

A 5.2-ml aliquot (0.0518 mol) of *N,N*-dimethylethanolamine and 100 ml methylene chloride was placed in a round bottom flask in an ice bath. At 0°C, 5 g (0.0518 mol) of fluoroacetyl chloride or chloroacetyl chloride were slowly added dropwise to the flask. The reaction proceeded and resulted in a clear liquid. The mixture was allowed to warm to room temperature. A solution of 2.07 g (0.0518 mol) NaOH dissolved in 20 ml water was added to the reaction flask. The mixture was stirred thoroughly and then placed in a separatory funnel. The methylene chloride layer was

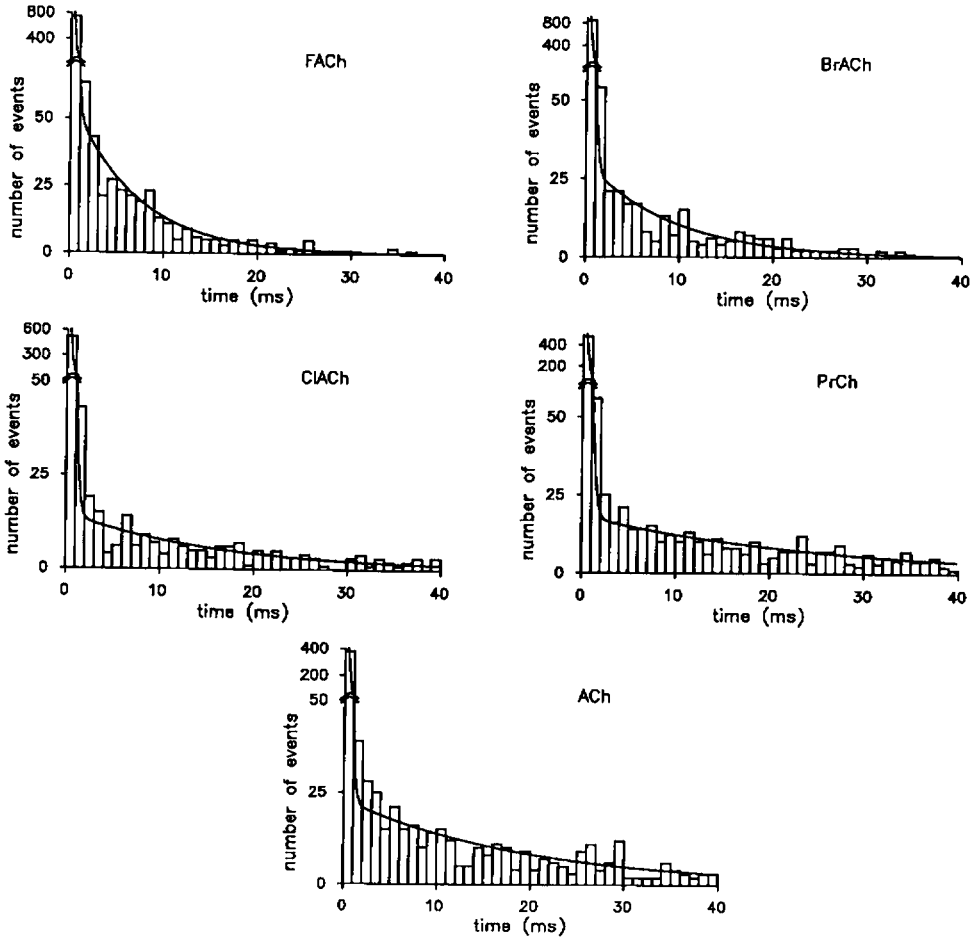

FIGURE 1 Examples of burst duration histograms for each of the five agonists. The curve through the bins was calculated from a two exponential model using maximum likelihood analysis of the original data as described in Materials and Methods. In each case, the concentration of agonist was 100 nM and the holding potential was 80 mV hyperpolarized relative to resting potential.

removed. Two additional methylene chloride extractions were performed and the organic layers were pooled. Small amounts of magnesium sulfate ($MgSO_4$) and decolorizing carbon were added to the organic solution to dry and decolorize it. The magnesium sulfate and decolorizing carbon were filtered out and the supernatant was collected in a 250-ml Ehrlenmeyer flask. Most of the methylene chloride was boiled off. Approximately 100 ml acetone was added and the remaining methylene chloride was then boiled off. A 3.22-ml aliquot (0.0518 mol) of iodomethane was added to the reaction mixture. A very viscous yellow liquid began to form on the bottom of the flask. The mixture was allowed to stand for 2 d until a yellow-white solid formed.

The crude solid was filtered under vaccuum with a Büchner filter and then washed with anhydrous ethyl ether. In the case of FACh, the crude solid was recrystallized from a 3:1 isopropyl alcohol/ethanol solution. For ClACh, the recrystallization was done in isopropyl alcohol alone. The crystals were then filtered and washed with small quantities of anhydrous ethyl ether. The crystals were allowed to dry and were removed from the filter. The crystals were stored dessicated at −20°C. The purity (>99%) after recrystallization was confirmed using ^{1}H-NMR spectroscopy at 200 MHz for both derivatives and ^{19}F-NMR at 400 MHz for FACh.

Materials

BC_3H-1 cells were obtained from American Cell Type Culture (Rockville, MD). Bromoacetyl bromide and *N,N*-dimethylethanolamine were purchased from Aldrich Chemical Co. (Milwaukee, WI). Fluoroacetyl chloride and chloroacetyl chloride were purchased from Alfa Products (Danvers, MA) and methyl iodide from Fisher Scientific Co. (Pittsburgh, PA). Propionylcholine iodide was purchased from Lancaster Synthesis Ltd. (Lancashire, UK).

RESULTS

Single Channel Data

Conductance. Two channel types were observed in these cells with conductances of 20 and 50 pS. The 20-pS channel was observed as frequently in the presence as in the absence of ACh and was not blocked by pretreatment with 1 μM α-bungarotoxin (α-Bgt). The appearance of the 50-pS channel was a function of agonist concentration and could be blocked by α-Bgt. For these reasons, only the 50-pS channel was assumed to be an AChR and the analysis described below was performed exclusively on this channel. The conductance of the channel did not vary with the type of agonist.

Open Times and Burst Durations. Apparent open times (τ) and burst durations (τ_b) were well fit by two exponentials for all five agonists. Representative burst duration histograms for each agonist at 100 nM are shown in Fig. 1. The time constants for the two components of burst durations (τ_b) and open times (τ) are summarized in Fig. 2. The long duration bursts (τ_{b2}) were shortest with FACh as the agonist and longest with PrCh (PrCh > ClACh > ACh > BrACh > FACh); and, the apparent elementary open times (τ_2) show a similar but less marked trend (PrCh > ACh ≥ ClACh > BrACh ≥ FACh). The differences between the open time and burst duration distributions are due to an increased number of apparent openings per burst for BrACh and ClACh (openings per burst: 1.32 ± 0.06 − FACh, 1.81 ± 0.3 − BrACh, 1.48 ± 0.1 − ACh, 1.87 ± 0.08 − ClACh, and 1.57 ± 0.09 − PrCh). The fast component of open times and burst durations also varied with the type of agonist (Fig. 2 *B*). Both ClACh and PrCh had significantly longer fast burst times (τ_{b1}) than ACh.

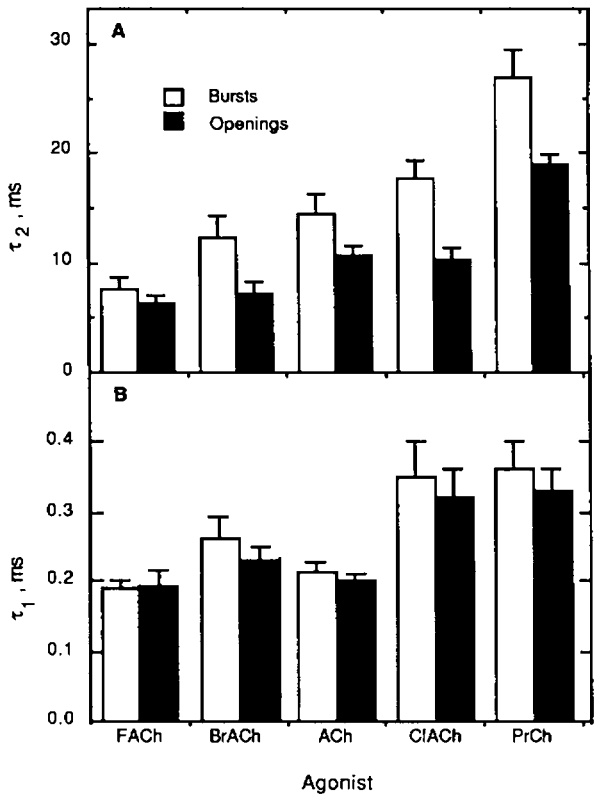

FIGURE 2 Average burst times and apparent open times for the long (*A*) and short (*B*) components of the burst durations. The averages represent 4–11 independent measurements for each agonist at 100 nM and 80 mV hyperpolarized relative to resting potential.

Closed Times. Control experiments at a wide range of ACh concentrations required four exponentials to fit the data adequately (Papke and Oswald, 1986). Because one of the components (τ_{c3}) represented <3% of the total distribution at 100 nM ACh, only three components were considered in this analysis. The two relatively fast components (τ_{c1} = 0.041 ± .003 ms and t_{c2} = 0.57 ± 0.12 ms) made up 29 ± 7% and 5.3 ± 0.6% of the distributions respectively at 100 nM ACh. The τ_{c3} component appears to be related to an interburst closed time, the properties of which are described elsewhere (Papke, 1987). The predominant long closed times were highly variable, presumably corresponding to variations in the numbers of channels in a patch. Excursions into the fast closed states occurred at the rate of 40.6 ± 4.6 per second of time in the long open state in the presence of 100 nM ACh.

Representative closed time histograms for the derivatives of ACh at 100 nM are shown in Fig. 3. The fastest closed times (τ_{c1}) for all four derivatives were significantly

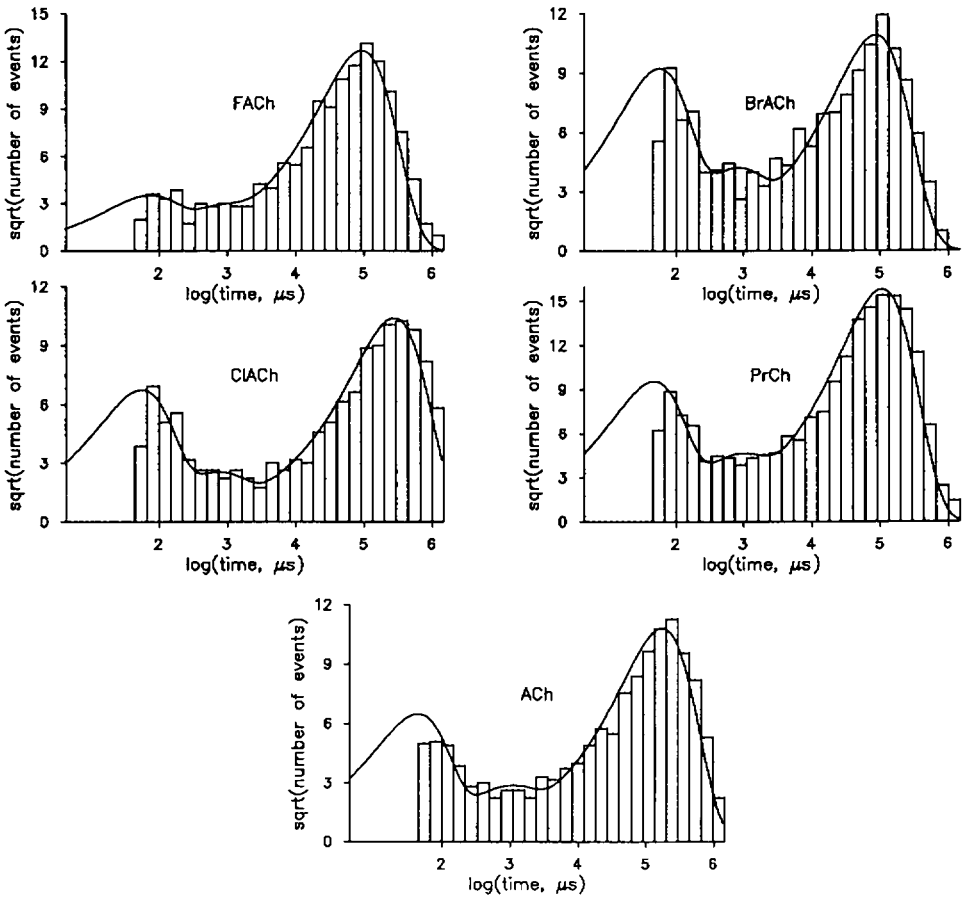

FIGURE 3 Examples of closed time histograms for each of the five agonists. The curve through the bins was calculated from a three exponential model using maximum likelihood analysis of the original data as described in Materials and Methods. The data are displayed as log transforms of time which permits the display of events occurring over widely distributed time intervals. As shown by Sigworth and Sine (1987), the maxima of such a transformed distribution represent time constants for each of the exponential components. In each case, the concentration of agonist was 100 nM and the holding potential was 80 mV hyperpolarized relative to resting potential. The solid lines through the bins were generated by the following equation:

$$f(x) = \sqrt{\sum_{i=1}^{n} a_i \exp\left[\ln t - \ln \tau_i - \exp\left(\ln t - \ln \tau_i\right)\right]},$$

where a_i is the fraction of total events in component i, τ_i is the time constant of component i, and n is the number of components.

($P < 0.05$) longer than that for ACh (Fig. 4 *A*) but were not significantly different from each other. The percentage of the distribution represented by τ_{c1} was significantly less for FACh than the other agonists. The intermediate closed time (Fig. 4 *B*) and the percentages of the distributions represented by τ_{c2} are not significantly different for the different agonists.

As was suggested by the burst analysis, the number of fast closures per long burst was significantly greater ($P < 0.05$) for ClACh than for ACh, and FACh had the fewest fast closures per burst. Expressed in terms of fast closures per second of open time (Fig. 4 *C*), the fastest rate was expressed by BrACh which may relate to the closing rate (α) of the channel when activated by this agonist. The frequency of τ_{c2} closures per second open time is also displayed (Fig. 4 *C*). Significantly fewer ($P < 0.05$) τ_{c2} closures per second were observed in ACh and PrCh than in any of the halogenated derivatives.

Kinetic Interpretation

Previous studies on a wide variety of nAChRs suggest that Scheme I can at least partially account for the observed single channel data (Colquhoun and Sakmann, 1985; Papke and Oswald, 1986). By concentrating on kinetics within the longer burst components, the simpler model shown

$$\begin{array}{ccccc} R + A \underset{k_{-1}}{\overset{k_{+1}}{\rightleftharpoons}} RA & + & A \underset{k_{-2}}{\overset{k_{+2}}{\rightleftharpoons}} RA_2 \\ \alpha' \Big\| \beta' & & \alpha \Big\| \beta \\ RA^* & & RA_2^* \end{array}$$

Scheme I

in Scheme II can account for the observed results. The goal is to relate the relaxations observed (e.g., τ_{c1}, τ_{c2}, etc.) to the kinetic constants implied by this scheme and then determine if

$$R + A \underset{k_{-1}}{\overset{k_{+1}}{\rightleftharpoons}} RA + A \underset{k_{-2}}{\overset{k_{+2}}{\rightleftharpoons}} RA_2 \underset{\alpha}{\overset{\beta}{\rightleftharpoons}} RA_2^*$$

Scheme II

correlations exist between these microscopic kinetic constants and aspects of the agonist structure. To make such correlations, we have made the following assumptions: (*a*) The long open time constants (τ_2) corrected for missed closures are inversely related to the closing rate of the channel ($1/\alpha$). This assumes that the analysis system can reconstruct lost short closures (see Methods). (*b*) The time constant associated with dwells in the RA_2 state is τ_{c1}. Based on Scheme II, τ_{c1} would be equal to $1/(\beta + k_{-2})$ and the number of such closures per burst (corrected for missed events and the number of fast closures in fast

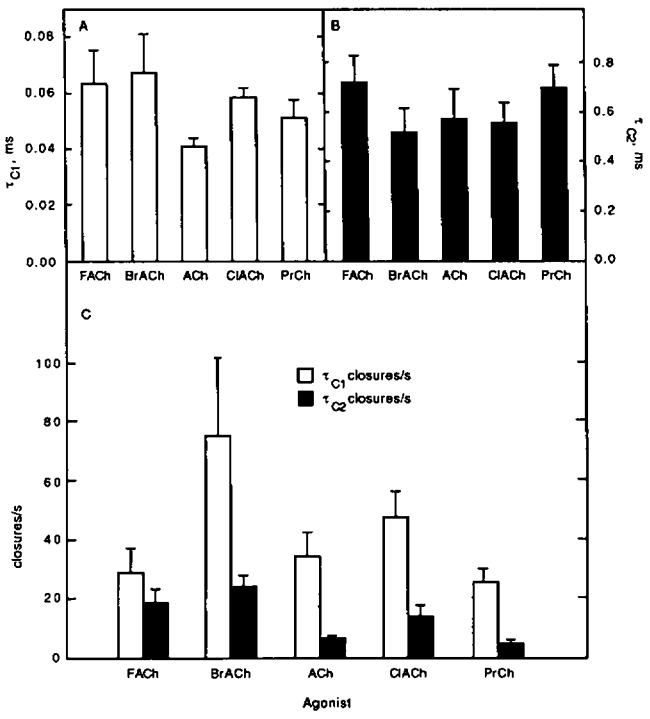

FIGURE 4 Parameter plots for closed time distributions. (*A*) Closed time constants for the short closures for each of the agonists. (*B*) Closed time constants for the intermediate closures for each of the agonists. (*C*) The number of closures per second of open time for the short and intermediate closures. As in Fig. 4, the concentration of agonist was 100 nM and the holding potential was 80 mV hyperpolarized relative to resting potential.

bursts) is β/k_{-2} (Colquhoun and Sakmann, 1985). The effect of this assumption on the results was explored by calculating k_{-2} and β assuming in one case that τ_{c1} represented RA_2 dwells and in the other that τ_{c2} represented such dwells (see Table I). Because τ_{c1} is more sensitive to the type of agonist (see Fig. 4 *A*) and because the values of β and k_{-2} calculated from this relation are in better agreement with previously published values (Colquhoun and Sakmann, 1985; Sine and Steinbach; 1986), we have used the values obtained from τ_{c1} in all subsequent calculations. (*c*) Approximations of the equilibrium dissociation constant K_D and forward binding rate (k_+) can be made by estimating the average number of channels per patch and the average burst frequency (i.e., number of long bursts per second) and assuming that no cooperativity in binding exists. Estimates of receptor distributions by quantitative autoradiography of $\alpha[^{125}I]$Bgt binding using representative cultures indicate that the receptors are, in general, diffusely distributed with a density of 73 ± 6 receptors/μm^2 (Rosenthal, J., and M. M. Salpeter, unpublished observations). Approximately 10% of the cell surface AChRs are clustered in patches with an approximately fivefold higher concentration than the remainder of the cell. The estimation of patch size from pipette resistance (2.3 ± 0.4 μm^2; Sakmann and Neher, 1983) indicated that ~170 ± 50 receptors were present per patch (except in the cases where "high density" clusters were inadventently patched—~10% of successful seals fell into this category and were excluded from the analysis). The assumption that binding to activatable receptors is noncooperative is consistent with a number of studies (see for example, Colquhoun and Sakmann, 1985) but has been questioned recently (Sine and Steinbach, 1987). This implies that

$$K_D = \frac{k_{+1}}{2k_{-1}} = \frac{2k_{+2}}{k_{-2}} \text{ and } k_+ \equiv k_{+1} = 2k_{+2}. \quad (1)$$

Given these assumptions and Eq. 2 (a modification of the expression derived by Sine and Steinbach, 1986), the values of K_D and k_+ for each agonist are given in Table I. The k_{-2} presented assumes that the dissociation rates for both of the agonist sites are the same. If they are not, the apparent value is biased toward the faster rate.

$$k_+ = \sqrt{\frac{\text{burst frequency} \times k_{-2}(k_{-2} + \beta)}{\beta\,(\text{agonist concentration})^2}}. \quad (2)$$

Relation between Microscopic Kinetics and Agonist Structure

Two general trends were observed as the nature of the agonist was changed at this single site: (*a*) the association and dissociation rates for ACh binding were correlated with the length of the bond on the acetyl group, and (*b*) the opening and closing rates of the channel were correlated with the distribution of charge in the substituted portion of the molecule.

TABLE I
MICROSCOPIC KINETIC PARAMETERS

Agonist	Values based on τ_{c1}		Values based on τ_{c2}		Values based on τ_{c1} and receptor density		
	β	k_{-2}	β	k_{-2}	K_D	α	k_+
	s^{-1}	s^{-1}	s^{-1}	s^{-1}	μM	s^{-1}	$M^{-1}s^{-1} \times 10^{-8}$
ACh	8,280 ± 1,400	18,389 ± 1,550	146 ± 40	1,717 ± 350	33	94	2.8
FACh	4,432 ± 881	14,454 ± 2,980	360 ± 74	1,390 ± 280	67	158	1.08
ClACh	8,125 ± 952	9,420 ± 377	373 ± 62	1,470 ± 200	64	97	0.73
BrACh	9,394 ± 2,500	10,540 ± 944	425 ± 120	2,230 ± 480	62	138	0.85
PrCh	7,652 ± 1,500	13,342 ± 1,200	135 ± 50	1,398 ± 210	61	62	1.09

ACh is a cation with the following structure:

$$(CH_2)_3\overset{+}{N}CH_2CH_2O\overset{O}{\overset{\|}{C}}CH_2R,$$

where R is a hydrogen. In this study we have varied R. Previous studies have shown that the important moieties, in terms of binding and activation, are the quaternary ammonium group, the carbonyl oxygen, and the distance between them (Beers and Reich, 1970). By substituting atoms and small atomic groups (i.e., methyl groups) at the R site, we felt that we were tuning the ACh structure in a very subtle way since the basic determinants established by Beers and Reich were not changed. As mentioned, the substituents at the R site were H, F, Cl, Br, and CH_3. There are two fundamental properties that characterize these groups: one is steric and the other is electrostatic. For the steric contribution, we use the bond length between the R group and the adjacent carbon atom. This is an easily obtainable quantity and it scales with any estimates of the "size" of the substituent atom or atomic group. For the electrostatic contribution we use the ionicity for this same bond. Ionicity is the percent ionic character of the bond and is a measure of the magnitude of the bond dipole moment.

Bond Length. The bond length between the methyl carbon of the acetyl group (see below) and the substituent atom (F, Br, Cl, H, C) was approximated as the bond length between methane and the corresponding substituent (Streitwieser and Heathcock, 1976). This approximation is justified because the bonds between carbon and substituted halogens are largely independent of other substituents on the methane molecule as long as the carbon remains in the sp^3 hybridization state. No significant correlation was observed between either α or β and the bond length ($P > 0.1$); however, correlations between k_{-2} ($P < 0.005$) and k_+ ($P < 0.05$) and the bond length were present. Both association and dissociation rates were inversely related to bond length (bond length: H < F < CH_3 < Cl < Br) as shown in Fig. 5, *A* and *B*. The equilibrium constant (K_D), on the other hand, changed very little between substituents (with the exception of ACh, which was twofold lower than the other compounds).

Ionicity. The percent ionic character of the bond (ionicity) was calculated from the Pauling electronegativities of carbon and the connected substituent atom or group as described by Atkins (1978). No correlation was observed between either k_{-2} or k_+ and the ionicity; however, α and β had opposite dependencies on the ionicity (α decreased, Fig. 6 *A*; β increased, Fig. 6 *B*). This suggests that the open channel state was energetically destabilized by increased ionic character of the bond.

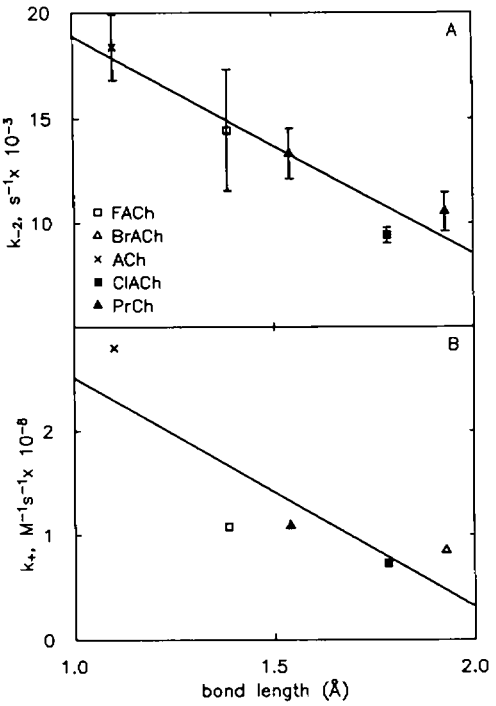

FIGURE 5 Relationship between the bond length between the acetyl carbon and the added substituent and (*A*) the dissociation rate of the agonist (k_{-2}) and (*B*) the association rate of the agonist (k_+). The lines drawn through the points were generated from a linear least squares fit to the data.

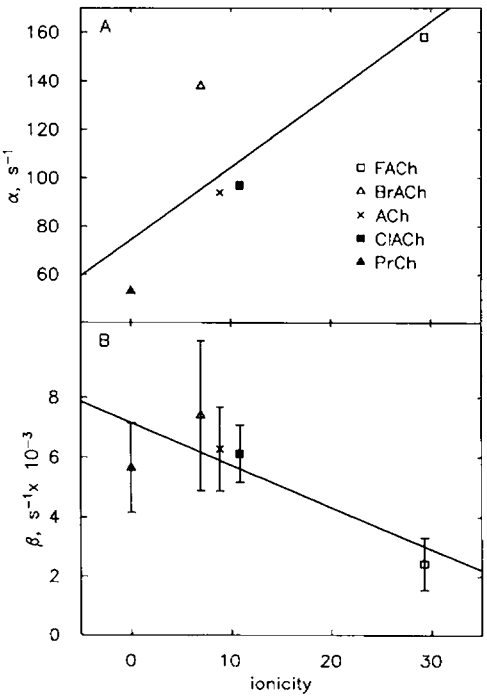

FIGURE 6 Relationship between the ionicity of the substituent bond and (*A*) the closing rate of the channel (α) and (*B*) the opening rate of the channel (β). The lines drawn through the points were generated from a linear least squares fit to the data.

DISCUSSION

The effects of a series of structurally related ACh derivatives on the microscopic kinetics of ACh binding and channel activation have been described. The following observations were made: (*a*) The apparent mean channel lifetime and burst duration of AChR channels change with modifications of the substituent on the acetyl group. (*b*) The value of the short closed time constant (τ_{c1}) and the percentage of the distribution that was made up by this component varied among agonists, suggesting that this component represents dwells in the RA_2 state. (*c*) Calculation of microscopic rate constants associated with ligand binding and channel activation suggest that (*i*) the association (k_+) and dissociation (k_{-2}) rates for ligand binding are decreased by increasing bond length (or substituent size) and (*ii*) the channel opening rate (β) is decreased and the channel closing rate (α) is increased by increasing ionic character (ionicity) of the bond between the acetyl carbon and the substituent.

We will now discuss the rate constants determined in terms of a kinetic model. To develop a kinetic model, it is important to assign the relative free energies of the three distinct states that correspond to a subset of the states from Scheme II:

$$RA + A \underset{k_{-2}}{\overset{k_{+2}}{\rightleftharpoons}} RA_2 \underset{\alpha}{\overset{\beta}{\rightleftharpoons}} RA_2^*.$$

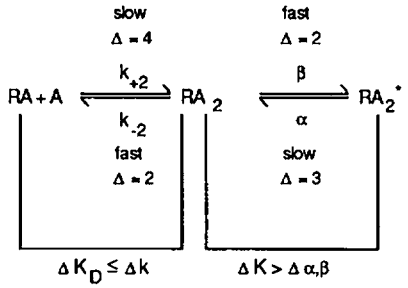

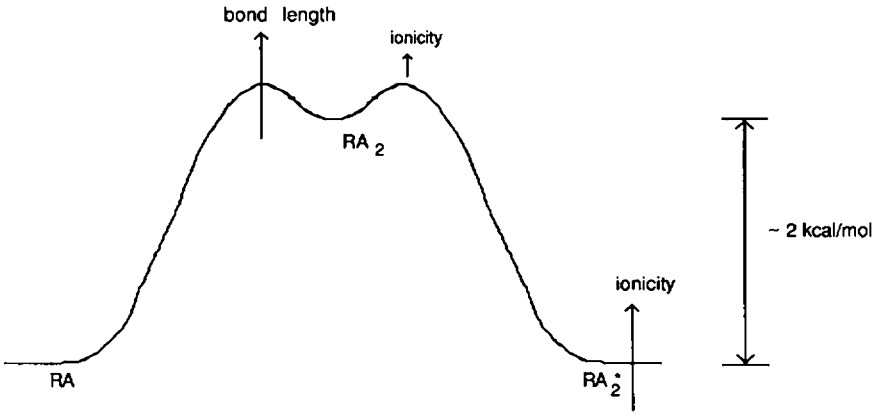

FIGURE 7 A qualitative picture of the energetics of cholinergic ligand binding and activation. The energy profile is drawn specifically for agonist at 1 μM, and the association rate constant indicated in the figure is shown as a pseudofirst order rate constant (i.e., the concentration of agonist is included in the constant so that the units are s^{-1}).

With all of the ligands, β and k_{-2} were always greater than α and k_+ (when k_+ is treated as a pseudofirst order rate constant by correcting for concentration and $k_+ = 2k_{+2}$) by at least two orders of magnitude. This indicates that the double liganded, closed state is higher in energy than the other two states by ~2 kcal/mol when the agonist concentration is 1 μM. The rate constants toward this state are comparable, suggesting that the singly liganded state and the open state have similar free energies.

Our experiments are always performed under equilibrium conditions which, by the principle of detailed balance, allow us to calculate equilibrium constants between the individual states. The equilibrium constant between the singly and doubly liganded states is, of course, the K_D for binding of the second agonist molecule. Because both k_+ and k_{-2} both follow the same dependence on the bond length (i.e., they both decrease with increasing bond length), this K_D does not change very much. For instance, k_+ changes by a factor of four over the range of agonists, whereas K_D only changes by a factor of two and only in the case of ACh. This suggests that the equilibrium between these two states does not change drastically, whereas both the forward and reverse rates do. Thus, we reason that the added substituent creates a steric effect that increases the energy of activation for ligand binding and unbinding.

Regarding the opening and closing of the ion channel, we find the opposite situation of the one described above. The forward and reverse rate constants have an opposite

dependence on the bond ionicity. This means that there is a substantial shift of the equilibrium properties of the system as a function of bond ionicity (i.e., as the ionicity increases, the equilibrium shifts to depopulate the open channel state). In contrast to the situation above, the rate constants, α and β, change by factors of three and two, respectively, whereas the equilibrium constant changes by a factor of seven.

These observations together form a qualitative picture of the energetics of cholinergic ligand binding and activation. Important considerations include the following: (*a*) the doubly liganded closed state is much higher in energy than its neighboring states, (*b*) the equilibrium between the singly and doubly liganded closed states is only weakly shifted by substituent bond length but the energy of the transition state increases due to steric effects, (*c*) the equilibrium between the doubly liganded closed and open states changes dramatically as a function of substituent bond ionicity, with a smaller increase in the energy of the transition state. We believe that points *b* and *c* indicate that the equilibrium shift between the open and closed states arises because of a destabilization of the open-channel state at high bond ionicity. The picture that emerges is shown in Fig. 7 with the regions labeled which are affected by the bond characteritics (of course, the equilibrium between the RA and the RA_2 states changes as a function of concentration).

The power of any theory is its ability to predict behavior of a system in situations that, as yet, are untested. From the model we have derived, we can predict the properties that are required at the acetyl end of an ACh-like molecule in order to create a potent agonist. Generally speaking, the steric factor should be large so that the agonist, once bound, remains bound. Additionally, the ionicity should be small so that the open-channel state is stabilized and thus remains open. The agonist, suberyldicholine, fulfills both of these characteristics and is found to be one of the most potent agonists. The open-channel lifetime is somewhat longer than that for ACh (Colquhoun and Sakmann, 1985) and the unbinding rate is much slower. Both of these properties are predicted by our model and are consistent with the high potency exhibited by this agonist.

These results suggest that it is possible, using microscopic kinetic measurements, to begin to assign changes in the structural characteristics of a ligand to changes in individual steps in a reaction scheme. Expanding such a strategy, one could potentially design ligands exhibiting specific characteristics such as extremely long open channel states or extremely high affinity for the ACh receptor. This should provide an effective strategy for the design of neuromuscular blockers as well as the design of useful agonists for probing the properties of ACh receptor–ion channel gating. Furthermore, such studies can shed considerable light on the three-dimensional structure of the ACh binding site.

The authors thank Dr M. M. Salpeter and J. Rosenthal for the quantitative autoradiographic analysis of $\alpha[^{125}I]$Bgt binding to BC_3H-1 cells, Dr. J. Wright for help with the hardware interface between the pulse code modulator and PDP 11/24, Drs. F. J. Sigworth and S. Sine for suggesting the use of log transform plot of closed time distributions, and Dr. G. A. Weiland and B. Coleman for comments on the manuscript.

This work was supported by grants from the Muscular Dystrophy Association, the National Institutes of Health (grant 1 R23 NS 18660-04 NEUB), and the Sloan Foundation to R. E. Oswald. G. Millhauser was supported by a National Institutes of Health postdoctoral fellowship (1 F32 NS07871-01).

Received for publication 3 April 1987 and in final form 16 September 1987.

REFERENCES

Atkins, P. W. 1978. Physical Chemistry. W. H. Freeman, New York.

Beers, W. H., and E. Reich. 1970. Structure and activity of acetylcholine. *Nature (Lond.).* 228:917–922.

Caceci, M. S., and W. P. Cacheris. 1984. Fitting curves to data: the simplex algorithm is the answer. *BYTE.* (May): 340–362.

Claudio, T., M. Ballivet, J. Patrick, and S. Heinemann. 1983. Nucleotide and deduced amino acid sequences of *Torpedo californica* acetylcholine receptor γ subunit. *Proc. Natl. Acad. Sci. USA.* 80:1111–1115.

Colquhoun, D., and A. G. Hawkes. 1981. On the stochastic properties of single ion channels. *Proc. R. Soc. Lond. B. Biol Sci.* 211:205–235.

Colquhoun, D., and A. G. Hawkes. 1982. On the stochastic properties of bursts of single ion channel openings and of clusters of bursts. *Philos. Trans. R. Soc. Lond. B. Biol. Sci.* 300:1–59.

Colquhoun, D., and A. G. Hawkes. 1983. The principles of the stochastic interpretation of ion-channel mechanisms. *In* Single-Channel Recording. B. Sakmann and E. Neher, editors. Plenum Publishing Corp., New York. 135–174.

Colquhoun, D., and B. Sakmann. 1981. Fluctuations in the microsecond time range of the current through single acetylcholine receptor channels. *Nature (Lond.).* 294:464–466.

Colquhoun, D., and B. Sakmann. 1985. Fast events in single-channel currents activated by acetylcholine and its analogues at the frog muscle end-plate. *J. Physiol. (Lond.).* 369:501–557.

Colquhoun, D., and F. J. Sigworth. 1983. Fitting and statistical analysis of single-channel records. *In* Single-Channel Recording. B. Sakmann and E. Neher, editors. Plenum Publishing Corp., New York. 191–264.

Damle, V. N., M. McLaughlin, and A. Karlin. 1978. Bromoacetylcholine as an affinity label of the acetylcholine receptor from *Torpedo californica. Biochem. Biophys. Res. Commun.* 84:845–851.

Devillers-Thiéry, A., J. Giraudat, M. Bentaboulet, and J. P. Changeux. 1983. Complete mRNA sequence of the acetylcholine binding α-subunit of *Torpedo marmorata* acetylcholine receptor: a model for the transmembrane organization of the polypeptide chain. *Proc. Natl. Acad. Sci. USA.* 80:2067–2071.

Giraudat, J., M. Denis, T. Heidmann, J. Y. Chang, and J. P. Changeux. 1986. Structure of the high-affinity binding site for noncompetitive blockers of the acetylcholine receptor: serine-262 of the δ subunit is labeled by [^{3}H]chlorpromazine. *Proc. Natl. Acad. Sci. USA.* 83:2719–2723.

Hamill, O. P., A. Marty, E. Neher, B. Sakmann, and F. J. Sigworth. 1981. Improved patch-clamp techniques for high-resolution current recording from cells and cell-free membrane patches. *Pfluegers Arch. Eur. J. Physiol.* 391:85–100.

Hansch, C. 1983. Quantitative approaches to pharmacological structure-activity relationships. *In* Structure Activity Relationships. C. J. Cavallito, editor. Pergamon, Oxford. 75–165.

Hucho, F., W. Oberthür, F. Lottspeich, and B. Wittmann-Liebold. 1986. A structural model of the ion channel of the nicotinic acetylcholine

receptor. *In* Nicotinic Acetylcholine Receptor: Structure and Function. A. Maelicke, editor. Springer-Verlag, Berlin. 115–127.

Imoto, K., C. Methfessel, B. Sakmann, M. Mishina, Y. Mori, T. Konno, K. Fukuda, M. Kurasaki, H. Buho, Y. Fujita, and S. Numa. 1986. Location of a δ-subunit region determining ion-transport through the acetylcholine-receptor channel. *Nature (Lond.)*. 324:670–674.

Kao, P. N., A. J. Dwork, R. R. J. Kaldany, M. L. Silver, J. Wideman. S. Stein, and A. Karlin. 1984. Identification of the α subunit half-cystine specifically labeled by an affinity reagent for the acetylcholine receptor binding site. *J. Biol. Chem.* 259:11662–11665.

Lindstrom, J., J. Merlie, and G. Yogeeswaran. 1979. Biochemical properties of acetylcholine receptor subunits from *Torpedo californica*. *Biochemistry*. 17:2035–2038.

Mishina, M., M. Kurasaki, T. Tobimatsu, K. Imoto, K. I. Tanaka, Y. Fujita, K. Fukuda, H. Takahashi, Y. Morimoto, T. Hirose, S. Inayama, T. Takahashi, M. Kuno, and S. Numa. 1985. Localization of functional regions of acetylcholine receptor α-subunit by site-directed mutagenesis. *Nature (Lond.)*. 313:364–369.

Neher, E., and B. Sakmann. 1976. Single-channel currents recorded from membrane of denervated frog muscle fibres. *Nature (Lond.)*. 260:799–802.

Noda, M., H. Takahashi, T. Tanabe, M. Toyasoto, S. Kikyotani, Y. Furutani, T. Hirose, H. Takashima, S. Inayama, T. Miyata, and S. Numa. 1983. Structural homology of *Torpedo californica* acetylcholine receptor subunits. *Nature (Lond.)*. 302:528–532.

Olsen, E. N., L. Glaser, J. P. Merlie, R. Sebanne, and J. Lindstrom. 1983. Regulation of surface expression of acetylcholine receptors in response to serum and cell growth in the BC_3H1 muscle cell line. *J. Biol. Chem.* 258:13946–13953.

Papke, R. L. 1987. The gating of single channel currents through the nicotinic acetylcholine receptors of BC_3H-1 cells: effects of agonists and allosteric ligands. Ph.D. Thesis, Cornell University, Ithaca, NY.

Papke, R. L., and R. E. Oswald. 1986. Effects of allosteric ligands on the gating of single channel currents in BC_3H-1 cells. *In* Nicotinic Acetylcholine Receptor: Structure and Function. A. Maelicke, editor. Springer-Verlag, Berlin. 243–257.

Raftery, M. A., M. W. Hunkapiller, C. D. Strader, and L. Hood. 1980. Acetylcholine receptor: complex of homologous subunits. *Science (Wash. DC)*. 208:1454–1457.

Rebek, J. 1987. Model studies in molecular recognition. *Science (Wash. DC)*. 235:1478–1484.

Reynolds, J. A., and A. Karlin. 1978. Molecular weight in detergent solution of acetylcholine receptor from *Torpedo californica*. *Biochemistry*. 17:2035–2038.

Sakmann, B., J. Patlak, and E. Neher. 1980. Single acetylcholine-activated channels show burst-kinetics in presence of desensitizing concentrations of agonist. *Nature (Lond.)*. 287:447–449.

Sakmann, B., and E. Neher. 1983. Geometric parameters of pipettes and membrane patches. *In* Single-Channel Recording. B. Sakmann and E. Neher, editors. Plenum Publishing Corp. New York. 37–52.

Sakmann, B., C. Methfessel, M. Mishina, T. Takahashi, T. Takai, M. Kurasaki, K. Fukuda, and S. Numa. 1985. Role of acetylcholine receptor subunits in gating of the channel. *Nature (Lond.)*. 318:538–543.

Sigworth, F. J., and S. M. Sine. 1987. Data transformation for improved display and fitting of single channel dwell time histograms. *Biophys. J.* 52:1047–1054.

Sine, S. M., and J. H. Steinbach. 1986. Activation of acetylcholine receptors on clonal mammalian BC_3H-1 cells by low concentrations of agonist. *J. Physiol. (Lond.)* 373:129–162.

Sine, S. M., and J. H. Steinbach. 1987. Activation of acetylcholine receptors on clonal mammalian BC_3H-1 cells by high concentrations of agonist. *J. Physiol. (Lond.)*. In press.

Spivak, C. E., T. M. Gund, R. F. Liang, and J. A. Waters. 1986. Structural and electronic requirements for potent agonists at a nicotinic receptor. *Eur. J. Pharmacol.* 120:127–131.

Spivak, C. E., B. Witkop, and E. X. Albuquerque. 1983. Potencies and channel properties induced by semirigid agonists of frog nicotine acetylcholine receptors. *Mol. Pharmacol.* 23:337.

Streitwieser, A., and C. H. Heathcock. 1976. Introduction to Organic Chemistry. Macmillan Publishing Co., New York.

White, M. M., K. Mixter-Mayne, H. A. Lester, and N. Davidson. 1985. Mouse-*Torpedo* acetylcholine receptor subunit hybrids expressed in *Xenopus* oocytes: functional homology does not equal sequence homology. *Proc. Natl. Acad. Sci. USA*. 82:4852–4856.